AD-A069 610 ARMY ELECTRONICS RESEARCH AND DEVELOPMENT COMMAND WS--ETC F/G 20/14
MICROWAVE EFFECTIVE EARTH RADIUS FACTOR VARIABILITY AT WIESBADE--ETC(U)
FEB 79 R RUBIO, D HOOCK

UNCLASSIFIED ERADCOM/ASL-TR-0023 NL

END
DATE
FILMED
7-79
DDC

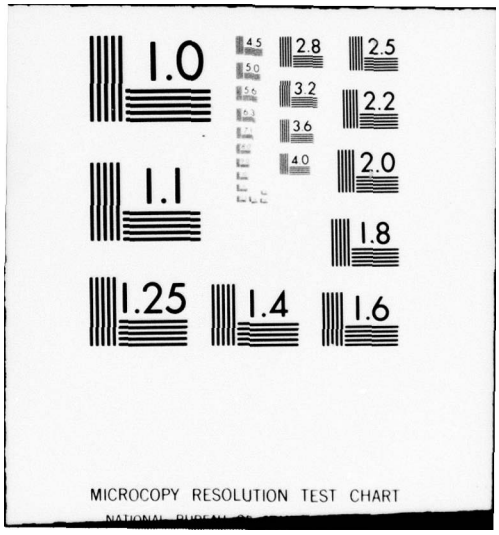
1.0
1.1
1.25
1.4
1.6
1.8
2.0
2.2
2.5
2.8
3.2
3.6
4.0
4.5
5.0
5.6
MICROCOPY RESOLUTION TEST CHART

ASL-TR-0023

AD
Reports Control Symbol
OSD - 1366

LEVEL II

MICROWAVE EFFECTIVE EARTH RADIUS FACTOR VARIABILITY AT WIESBADEN AND BALBOA

AD A069610

FEBRUARY 1979

By

ROBERTO RUBIO
ATMOSPHERIC SCIENCES LABORATORY
White Sands Missile Range, NM 88002

DON HOOCK
PHYSICAL SCIENCES LABORATORY
New Mexico State University
Las Cruces, NM 88003

Approved for public release; distribution unlimited

US Army Electronics Research and Development Command
Atmospheric Sciences Laboratory
White Sands Missile Range, NM 88002

NOTICES

Disclaimers

The findings in this report are not to be construed as an official Department of the Army position, unless so designated by other authorized documents.

The citation of trade names and names of manufacturers in this report is not to be construed as official Government indorsement or approval of commercial products or services referenced herein.

Disposition

Destroy this report when it is no longer needed. Do not return it to the originator.

SECURITY CLASSIFICATION OF THIS PAGE *(When Data Entered)*

REPORT DOCUMENTATION PAGE

READ INSTRUCTIONS BEFORE COMPLETING FORM

1. REPORT NUMBER: ASL-TR-0023
2. GOVT ACCESSION NO.
3. RECIPIENT'S CATALOG NUMBER

4. TITLE *(and Subtitle)*: (6) Microwave Effective Earth Radius Factor Variability at Wiesbaden and Balboa
5. TYPE OF REPORT & PERIOD COVERED: R&D Technical Report
6. PERFORMING ORG. REPORT NUMBER

7. AUTHOR(s): (10) Roberto Rubio, Atmospheric Sciences Laboratory
Don Hoock, Physical Sciences Laboratory
New Mexico State University, Las Cruces, NM 88003
8. CONTRACT OR GRANT NUMBER(s)

9. PERFORMING ORGANIZATION NAME AND ADDRESS: Atmospheric Sciences Laboratory
White Sands Missile Range, New Mexico 88002
10. PROGRAM ELEMENT, PROJECT, TASK AREA & WORK UNIT NUMBERS: (16) DA Task No. 1L162111AH71

11. CONTROLLING OFFICE NAME AND ADDRESS: US Army Electronics Research and Development Command
Adelphi, MD 20783
12. REPORT DATE: (11) February 1979
13. NUMBER OF PAGES: 31

14. MONITORING AGENCY NAME & ADDRESS *(if different from Controlling Office)*: (9) Technical rept.,
15. SECURITY CLASS. *(of this report)*: UNCLASSIFIED
15a. DECLASSIFICATION/DOWNGRADING SCHEDULE

16. DISTRIBUTION STATEMENT *(of this Report)*

Approved for public release; distribution unlimited. (12) 34 p.

17. DISTRIBUTION STATEMENT *(of the abstract entered in Block 20, if different from Report)*

(14) ERADCOM/ASL-TR-0023

18. SUPPLEMENTARY NOTES

19. KEY WORDS *(Continue on reverse side if necessary and identify by block number)*

Refractivity variability
Microwave
Confidence intervals

20. ABSTRACT *(Continue on reverse side if necessary and identify by block number)*

This report describes the variability of the microwave (3 to 30 GHz) circuit design parameter, effective earth radius factor, at two sites which served as test cases: Balboa, Panama, and Wiesbaden, Germany. Median effective earth radius factors, K, derived from meteorological data for the first 100 m altitude at these two sites, were 1.32 for Wiesbaden and 1.68 for Balboa. Median K factors for 84 other world localities are included in table 1. Numerous medians differ considerably from the K = 4/3 standard. K factor variability at Balboa → next page

DD FORM 1 JAN 73 1473 EDITION OF 1 NOV 65 IS OBSOLETE

410 663

SECURITY CLASSIFICATION OF THIS PAGE *(When Data Entered)*

20. ABSTRACT (cont)

and Wiesbaden is illustrated with sets of equivalent earth profile curves enclosing 68.3, 95.4, 99.7, and 100 percent of the data and by K factor cumulative distribution functions bounded by respective 90 and 99 percent confidence limits. Effective earth radius factors were highly variable, particularly at Balboa, where the meteorological variability is high within the first 100 m altitude.

ERRATA SHEET

ASL-TR-0023

MICROWAVE EFFECTIVE EARTH RADIUS FACTOR
VARIABILITY AT WIESBADEN AND BALBOA

Page 4 — Fifth line from bottom of page. Delete sentence: "The above procedure shows that $\Delta N/\Delta h$ is assumed to be linear in the first 100 m of altitude."

Page 6 — Figure 1. Abscissa label should read: "N units/km for first 100 m above ground level."

Page 14 — Figure 5. Abscissa division markers are missing. Markers should be included as shown in figure 4.

Page 18 — Equation (13). The letter S should be lowercase s.

CONTENTS

	Page
INTRODUCTION	2
METEOROLOGICAL AND REFRACTIVITY DATA	3
EFFECTIVE EARTH CURVATURES	5
EFFECTIVE EARTH RADIUS FACTOR DISTRIBUTION FUNCTIONS	13
CONCLUSIONS	19
REFERENCES	21

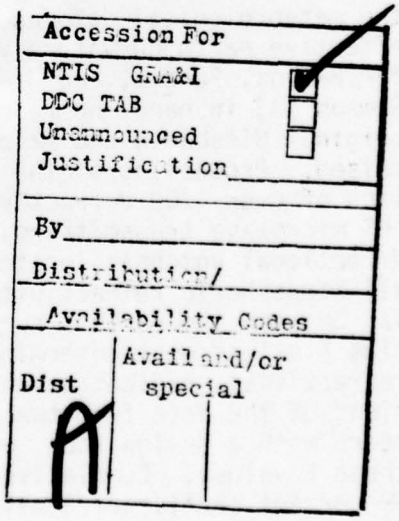

INTRODUCTION

The US Army Communications Command (USACC), under the provisions of AR 10-13, is responsible for performing electromagnetic wave propagation engineering services for agencies of the US Army and other government offices and for maintaining the operational electromagnetic compatibility (EMC) program area [1]. These responsibilities have been functionally assigned to the Electromagnetic Engineering Office (EMEO) located within the US Army Communications-Electronics Engineering Installation Agency. Under this mandate one of the tasks the EMEO performs is to provide engineering consultation and RF system performance analysis and design for line-of-sight (LOS) super high frequency (SHF, 3 to 30 GHz) communications links [1]. For each SHF link, transmitter and receiver spacing, antenna sizes and heights, an all-year median path attenuation figure, and a percentage of time during which a specified service should be achieved are all determined as part of the circuit design. To determine the above quantities, an average radio wave refractivity gradient is usually assumed, converted to an effective earth curvature correction, and entered into the calculations. Tropospheric radio wave refraction gradients, however, are a function of atmospheric relative humidity, temperature, and pressure, three highly variable parameters. Recognizing the variability of refractivity gradients as a function of time and world locality, the EMEO requested that the Atmospheric Sciences Laboratory (ASL) perform the statistics which delineate the range of effective earth radius values to be encountered at specified world localities by electromagnetic waves used in SHF systems [2].

This report describes the mathematical procedure used in interpreting the meteorological data and the statistical technique employed to derive effective earth curvature variability and presents the results obtained for Balboa, Panama, and Wiesbaden, Germany. The fundamental ideas of Samson [3] in handling refractivity gradients were studied; then his original Wiesbaden and Balboa meteorological data were obtained and processed. Processing of the meteorological data involved the determination of over 4700 refractivity gradients at each station. Since most LOS microwave transmitters, repeaters, and receivers employ high-gain directional antennas located within the first 100 m above ground level, all atmospheric refractivity gradients derived here are for that interval between the earth's surface and 100 m altitude. Effective earth radius K values were determined corresponding to the median value of the refractivity gradient at each station and to selected percentile deviations of the data from the median. To provide US Army microwave engineers with a design tool, equivalent earth profiles were plotted for these K values. Cumulative distribution functions of K and the 90 and 99 percent confidence limits for each K value were also determined from the data. Details of the aforementioned analysis are included as part of this report.

METEOROLOGICAL AND REFRACTIVITY DATA

The primary sources of meteorological data, excluding surface observations, are those measurements of relative humidity, pressure, and temperature obtained with standard balloon-borne radiosondes in use throughout the world. Radiosonde observations of temperature, pressure, and relative humidity are reported at fixed atmospheric pressure levels termed "mandatory levels" and at "significant levels." Significant levels are those where an appreciable change in temperature or relative humidity as a function of altitude occurred before the balloon reached the next mandatory level. Consequently, mandatory levels differ in altitude because of differences in terrain elevation at each sounding station. Significant levels differ in altitude due to the variable temperature lapse rates encountered during the year. Normally the first mandatory level or significant level above the surface is at an altitude greater than 100 m. Therefore to calculate refractivity at 100 m altitude, and subsequently the refractivity gradient for that interval, an interpolation scheme had to be employed which utilizes the calculated refractivity values obtained from the meteorological measurements at the surface and at the lowest mandatory level.

The expression for radio wave refractivity in the lower troposphere, for frequencies up to 30 GHz, is well established [4] and is of the form:

$$N = 77.6 \frac{P}{T} + 3.73 \times 10^5 \frac{e}{T^2} \qquad (1)$$

where P is the total atmospheric pressure in millibars, T is absolute temperature in degrees Kelvin, and e is the partial pressure of water vapor in millibars. N is in units of refractivity, related to the usual index of refraction n by $N = 10^6(n - 1)$. In equation 1, the quantity 77.6 P/T is normally referred to as the "dry term," while the quantity $3.73 \times 10^5 e/T^2$ is called the "wet term." Accordingly, the refractivity may be expressed as

$$N = N_D + N_W \, , \qquad (2)$$

where

$$N_D = 77.6 \, P/T \, , \qquad (3)$$

$$N_W = 3.73 \times 10^5 e/T^2 \, . \qquad (4)$$

Variations in refractivity as a function of altitude have been shown to follow an exponential function [5] of the form

$$N_D = A_D\, e^{-B_D h_1} , \tag{5}$$

$$N_w = A_w\, e^{-B_w h_1} . \tag{6}$$

Since the assembled meteorological data allow one to calculate N_D and N_w at the earth's surface and at the first mandatory altitude of h_1, solutions for the parameters A_D, A_w, B_D, and B_w were obtained and substituted into equations 5 and 6. Subsequently equations 5 and 6 were summed to yield the following refractivity interpolation equation:

$$N(h) = N_D(h_o)\left[\frac{N_D(h_o)}{N_D(h_1)}\right]^{-\frac{h}{h_1}} + N_w(h_o)\left[\frac{N_w(h_o)}{N_w(h_1)}\right]^{-\frac{h}{h_1}} , \tag{7}$$

where

$N(h)$ = Total refractivity at altitude h,

$N_D(h_o)$ = Dry term refractivity at earth's surface, h_o,

$N_D(h_1)$ = Dry term refractivity at altitude h_1 for which data is available,

$N_w(h_o)$ = Wet term refractivity at earth's surface, h_o,

$N_w(h_1)$ = Wet term refractivity at altitude h_1 for which data is available.

Each interpolation yielded a refractivity magnitude at an altitude of 100 m, which when subtracted from the refractivity magnitude obtained at the earth's surface, provided the desired refractivity gradient, $\Delta N/\Delta h$. The above procedure shows that $\Delta N/\Delta h$ is assumed to be linear in the first 100 m of altitude. For the locality of Balboa, Panama, 4917 refractivity gradients were computed with radiosonde measurements of the period from 1951 to 1956. During the sunrise atmospheric heating and sunset cooling time periods, refractivity gradients exhibit maximum

variability and definite changes in absolute magnitude. Thus in an analysis of this type, it is desirable to have a meteorological sample of the sunrise and sunset periods included. However, of the total data set, only 380 samples were representative of near sunset or sunrise hours; the remainder of the data set consists of a balanced mixture of totally night or daytime meteorological data. For Wiesbaden, Germany, 4798 refractivity gradients were derived from data recorded during the period 1951 to 1957. All Wiesbaden meteorological data are from either daytime or night radiosonde measurements; no sunrise or sunset samples were available. Consequently, the variability results to be presented here are inherently conservative.

Ordinal listings of the 100-m refractivity gradients for Balboa and Wiesbaden were compiled and the median refractivities of -64 units/km and -38 units/km, respectively, were obtained. Initial attempts to work with average refractivity gradients and deviations from the average value proved meaningless because the frequency distribution of the refractivity gradients was found to be non-Gaussian. Figures 1 and 2 are refractivity gradient histograms which approximate the frequency distributions at Balboa and Wiesbaden. These figures show that the distribution is non-Gaussian or at least that the sample was insufficient to a Gaussian distribution. Therefore, nonparametric statistics were employed to determine a median value and percentile distributions about the median. Annotated on the histograms are the median values and percentile deviations from the median obtained directly from the ordinal listing. The 34th and 47.5th percentile deviations denote how 68 and 95 percent of the data are distributed about the median. For Balboa, 95 percent of the gradient data is within -202 and -1 units/km; while for Wiesbaden, 95 percent of the gradients have values ranging from -86 to +16 units/km.

EFFECTIVE EARTH CURVATURES

Radio transmission path profiles used to design microwave communications links must account for the earth's curvature and radio beam refractivity. To expedite circuit design work, the radio beam refraction is normally combined with the earth's curvature to define an effective earth radius usually designated as Kr, where r is the true earth radius and K is the atmospheric refraction dependent modification factor. Depiction of the earth with an effective earth radius of Kr allows the radio beam to be drawn as a straight line as shown in figures 3a and 3b. To further facilitate path profile plotting, both curves can be transformed to a flat earth reference frame and a radio wave beam with curvature Kr as shown in figure 3c or 3d. Variations in the K factor, induced by meteorological changes, may then be depicted by several plots representing the range of probable Kr magnitudes.

In this section the equations used to derive all the K factors, the median K, percentile deviations from the median K, and equivalent earth profile curves as shown in figure 3d are described. Actual values and

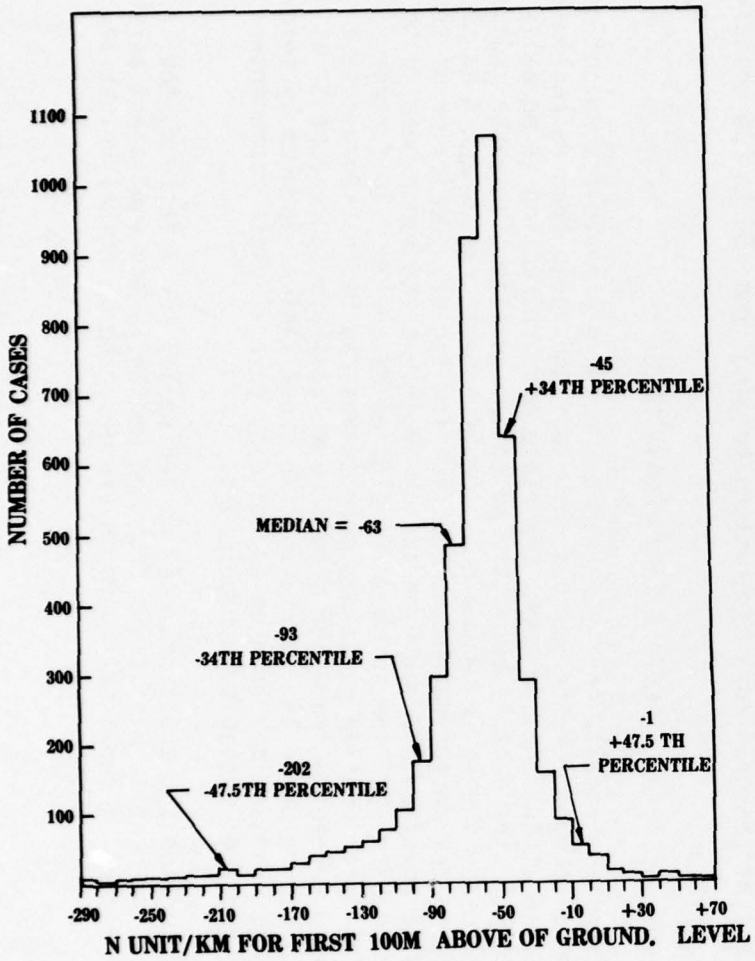

Figure 1. Balboa, Panama, refractivity gradient histogram.

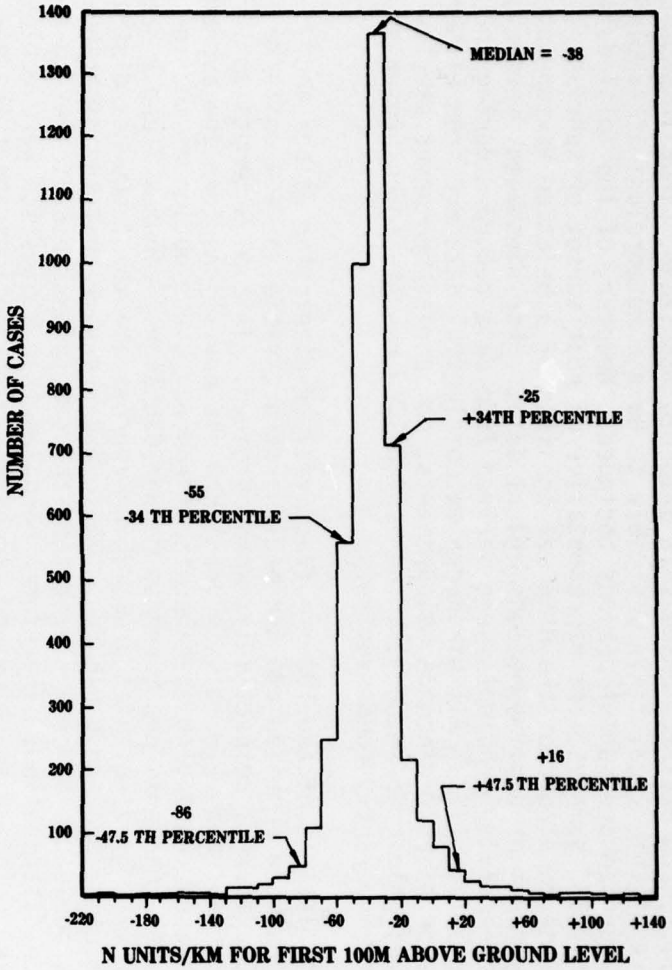

Figure 2. Wiesbaden, Germany, refractivity gradient histogram.

$\left(\frac{\Delta N}{\Delta h}\right)_M$ = Median $\Delta N/\Delta h$,

$\left(\frac{\Delta N}{\Delta h}\right)_P$ = P^{th} percentile value of $\Delta N/\Delta h$ obtained directly from ordinal listing

Equivalent earth profile curves, like those shown in figures 3c and 3d, were constructed by using the simple geometric relationship [6]

$$h = \frac{2}{3}\frac{d^2}{K} \quad , \tag{11}$$

where

h = height above path center at horizontal distance d,

d = horizontal distance from path center,

K = equivalent earth radius factor.

Graphs employing relationship shown in equation 11 display the variability of radio beam refractivity for expected magnitudes of K determined from statistical analysis using pertinent meteorological data.

Employing equation 9, median K values of 1.68 and 1.32 were calculated for Balboa and Wiesbaden, respectively. Note here that the Wiesbaden K value of 1.32 is in agreement with the K = 4/3 value conventionally used throughout the world; however, the Balboa median differs significantly from 4/3. Reference 5 provides a catalog of median refractivity gradients for 86 world locations. These gradients have also been converted to median K values employing equation 9 and are listed in alphabetical order in table 1.

Percentile deviations from the median equivalent to standard deviation percentage ranges commonly used in Gaussian distributions (σ, 2σ, etc.) were identified in the refractivity gradient ordinal listing and used in equation 10 to compute the corresponding K values. The median K values and the K's obtained for the 68.3th, 95.4th, 99.7th, and 100th percentile

TABLE 1. EQUIVALENT EARTH RADIUS FACTOR MEDIANS

City	State/Country	Approximate Geographic Coordinates		Median K
Abidjan,	Ivory Coast	5 N	4 W	K = 1.35
Aden,	Yemen	13 N	45 E	K = 1.55
Anchorage,	Alaska, US	61 N	150 W	K = 1.39
Aloulef,	Algeria	27 N	1 E	K = 1.35
Argentia,	Newfoundland	47 N	54 W	K = 1.32
Athens,	Greece	38 N	24 E	K = 1.38
Atlanta,	Georgia, US	34 N	84 W	K = 1.78
Balboa,	Canal Zone	9 N	80 W	K = 1.68
Bangui,	Central African Republic	4 N	19 E	K = 1.73
Barrow,	Alaska, US	71 N	157 W	K = 1.33
Bitburg,	Germany	50 N	7 E	K = 1.34
Bordeaux,	France	45 N	1 E	K = 1.62
Brownsville,	Texas, US	26 N	97 W	K = 1.65
Brussel,	Belgium	51 N	4 E	K = 1.54
Calcutta,	India	23 N	88 E	K = 2.38
Charleston,	South Carolina, US	33 N	80 W	K = 1.51
Chitta,	USSR	52 N	113 E	K = 1.37
Clark Field,	Luzon, Philippines	15 N	121 E	K = 1.52
Cocoa Beach,	Florida, US	28 N	81 W	K = 1.6
Columbia,	Missouri, US	39 N	92 W	K = 1.5
Coral Harbor,	Northwest Territories, Canada	64 N	83 W	K = 1.43
Curacao,	Netherlands West Indies	12 N	69 W	K = 1.67
Dakar,	Senegal	15 N	17 W	K = 157.0
Denver,	Colorado, US	40 N	105 W	K = 1.34
El Paso,	Texas, US	32 N	106 W	K = 1.44
Ft. Lamy,	Chad	12 N	15 E	K = -78.5
Ft. Smith,	Northwest Territories, Canada	61 N	112 W	K = 1.35
Ft. Trinquet,	Mauritania	25 N	12 W	K = 1.45
Gibraltar	(British Colony) Spain	36 N	5 W	K = 1.6
Gross Rohrheim,	Germany	50 N	8 E	K = 1.54
Guantanamo,	Cuba	20 N	75 W	K = 1.45
Gur'Yey,	Kazah, USSR	47 N	52 E	K = 1.34
Hannover,	Germany	52 N	10 E	K = 1.47
Hilo,	Hawaii, US	20 N	155 W	K = 1.65
Hong Kong	(British Colony) China	22 N	114 E	K = 1.59

Table 1 (cont)

City	State/Country	Approximate Geographic Coordinates		Median K
Isachsen,	NM Territories, Canada	79 N	103 W	K = 1.45
Joliet,	Illinois, US	41 N	88 W	K = 1.51
Karaganda,	Kazakhstan, USSR	50 N	78 W	K = 1.33
Key West,	Florida, US	25 N	82 W	K = 1.52
Khartom,	Sudan	16 N	33 E	K = 1.34
Koror Island,	Pacific	7 N	134 E	K = 1.94
La Coruna,	Spain	43 N	8 W	K = 1.34
Long Beach,	California, US	34 N	118 W	K = 1.44
Long Xuyen,	Viet Nam (Only 1 month of data available; morning hours)	10 N	105 E	K = 1.0
L'Vov,	Ukrain, USSR	50 N	24 E	K = 1.4
Madrid,	Spain	40 N	4 W	K = 1.35
Majuro,	Marshall Islands, Pacific	7 N	171 E	K = 1.64
Mazatlan,	Mexico	23 N	106 W	K = 1.8
Miami,	Florida, US	26 N	80 W	K = 1.65
Midway Island,	Pacific	28 N	177 W	K = 1.54
Moscow,	USSR	56 N	38 E	K = 1.34
Muharraq,	Bahrain (Persian Gulf)	26 N	51 E	K = -31.4
New Delhi,	India	29 N	77 E	K = 2.57
New York,	New York, US	41 N	74 W	K = 1.34
Niamay,	Niger	13 N	2 E	K = 5.81
Nicosia,	Cyprus	35 N	33 E	K = 1.32
Oakland,	California, US	38 N	122 W	K = 1.48
Odessa,	Ukraine, USSR	46 N	31 E	K = 1.4
Okhotsk,	Khabarovsk Territory, USSR	59 N	143 E	K = 1.38
Ostersund,	Sweden	63 N	15 E	K = 1.33
Palma,	Majorca	40 N	3 E	K = 1.29
Port Lyautey,	Morocco	34 N	7 W	K = 1.6
Saigon,	Viet Nam	11 N	107 E	K = 1.8
San Diego,	California, US	33 N	117 W	K = 1.5
San Juan,	Puerto Rico	18 N	66 W	K = 1.8
Seattle,	Washington, US	47 N	122 W	K = 1.41
Shemya,	Alaska, US	53 N	174 E	K = 1.3
Ship "C"	(Atlantic Ocean)	53 N	35 W	K = 1.34
Ship "K"	(Atlantic Ocean)	45 N	16 W	K = 1.41
Ship "M"	(Norwegian Sea)	66 N	2 E	K = 1.34
Ship "V"	(Pacific Ocean)	34 N	164 E	K = 1.65
Singapore	(South of Malay Peninsula)	1 N	104 E	K = 1.99
Stuttgart,	Germany	49 N	9 E	K = 1.47
Swan Island,	West Indies	17 N	84 W	K = 1.62

Table 1 (cont)

City	State/Country	Approximate Geographic Coordinates		Median K
Syktyvkay	Komi, USSR	62 N	51 E	K = 1.33
Tampa	Florida, US	28 N	83 W	K = 1.65
Tan An	Viet Nam	11 N	106 E	K = 1.8
Tashkent	U Bekistan, USSR	41 N	69 E	K = 1.47
Tateno	Japan	36 N	140 E	K = 1.48
Tatoosh Island	Washington, US	48 N	125 W	K = 1.43
Tura	Krasnoyarsk Territory, USSR	64 N	100 E	K = 1.45
Verkhoyansk	North Yakut, USSR	67 N	133 E	K = 1.59
Vladivostok	USSR	43 N	133 E	K = 1.39
Wake Island	Pacific	19 N	167 E	K = 1.85
Washington	DC, US	39 N	77 W	K = 1.34
Wiesbaden	Germany (Federal Republic)	50 N	8 E	K = 1.32

regions about the Balboa and Wiesbaden median, respectively, are tabulated in figures 4 and 5. Inspection of the K column in figures 4 and 5 reveals three ranges of the K magnitudes which are of interest: $0 < k < 1$, $1 \leq K < \infty$, and K negative.

These K data sets indicate, respectively, that the radio beam curves upward away from the earth, downward with a curvature less than the earth's, and downward with a curvature greater than the earth's. For Balboa, $0 < K < 1$ occurred about 2.5 percent of the time, $1 \leq K \leq \infty$ occurred about 93 percent of the time, and K negative occurred the remaining 4.5 percent. Note that the extreme K factors at Balboa for this 5-year period were +0.39 and -0.10. At Wiesbaden, $0 < K < 1$ occurred 4.6 percent of the time, $1 \leq K \leq \infty$ occurred 95.2 percent of the time, and K was negative the remaining 0.2 percent. The extreme K factors for Wiesbaden, +0.36 and -0.73, were not as severe as those found at Balboa.

Equivalent earth profile curves for each of the listed K values for Balboa and Wiesbaden are also included in figures 4 and 5. These sets of profiles were constructed with the use of equation 11 after the origin was chosen, quite arbitrarily, 275 ft above the abscissa which was designated as the flat earth surface. The coordinates (d,h) for a selected K of interest, identify the location of the radio terminals. Clearance requirements above the flat earth reference are usually dictated by the height of obstructing terrain and edifices. Since the plots of figures 4 and 5 represent the percentile deviations from the median K values, these curves identify the expected variability of radio beam refraction along the path and particularly at the radio terminal. The plots labeled +4 and -4, accordingly, represent the maximum earth - beam divergence and maximum downward refractivity which might occur. Figures 4 and 5 show, again, that radio beam dispersion is greater at Balboa than at Wiesbaden. For example, if a transmission path of 32 miles is selected, the radio beam axis will remain within approximately +15 ft and -20 ft of the median K path 63.3 percent of the time and +60 ft and -55 ft 95.4 percent of the time at Wiesbaden, Germany, while at Balboa, Panama, the beam axis varies about the median K path +20 ft and -35 ft 63.3 percent of the time and +70 ft and -155 ft, 95.4 percent of the time. These radio beam variability graphs may also be used to graphically approximate the system downtime due to atmospheric refractivity once the path length, antenna size and tower height, beam width, and signal-to-noise ratio are specified.

EFFECTIVE EARTH RADIUS FACTOR DISTRIBUTION FUNCTIONS

Design of high reliability microwave circuits requires not only a knowledge of the median effective earth radius factor, K, but also some measure of its distribution and the degree of confidence associated with each distribution. Thus, cumulative distribution functions for the

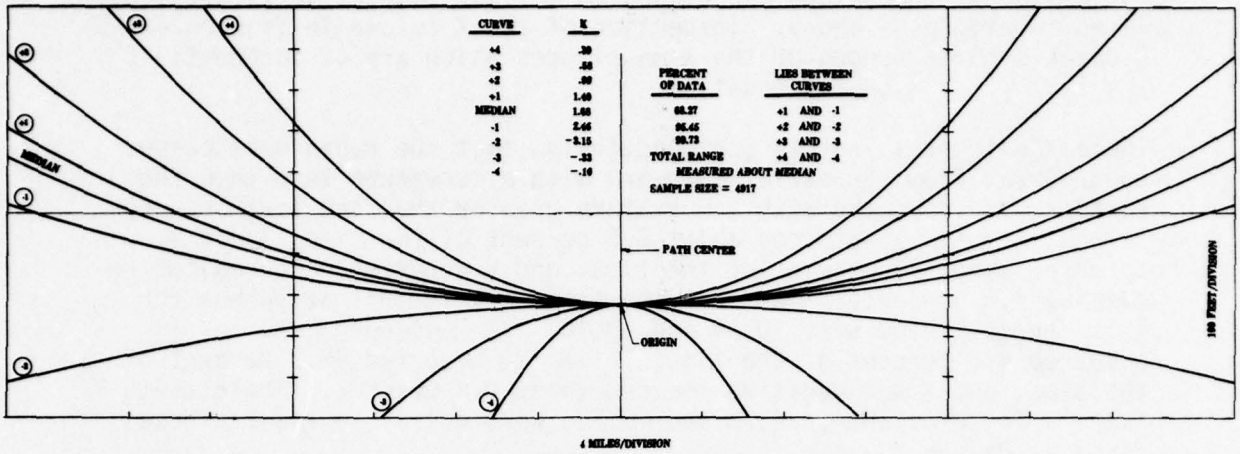

Figure 4. Profiles of combined earth and refractivity curvatures based on K median and percentile deviation values derived from Balboa, Panama, meteorological data.

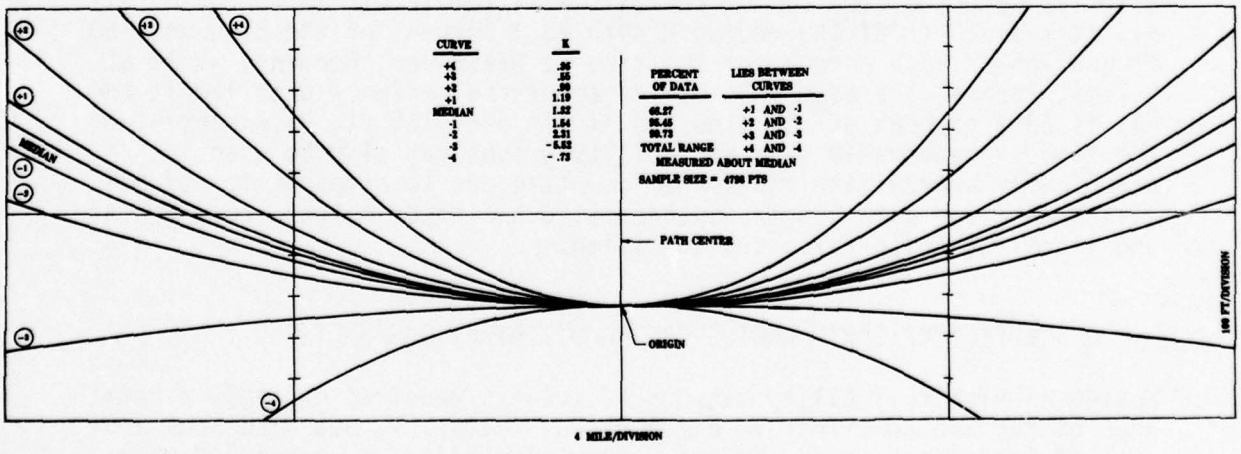

Figure 5. Profiles of combined earth and refractivity curvatures based on K median and percentile deviation values derived from Wiesbaden, Germany, meteorological data.

Balboa and Wiesbaden effective earth radius factors were constructed along with the derived 90 and 99 percent confidence interval for each function. K factor cumulative distributions were ordered from the smallest positive K value to infinity, abruptly changed to minus infinity, and then ordered towards the smallest negative K, all as a function of the percent of total cases. This arrangement is plotted in the center graphs of figures 6 and 7, and although it differs drastically from the conventional smallest to largest number cumulative distributions, it does depict the degree and direction of actual radio beam bending without introducing physical discontinuities. Near-infinite K values occur a significant portion of the time. This arrangement also places the median K value near the graph center and relegates the rarer extreme refractivity cases to the plot edges. Figures 6 and 7 are not all-inclusive because the few extreme valued K factors encountered called for an unnecessarily large graph. Instead, these K factors and the respective cumulative percentages are listed in table 2.

By selection of a specific K_p magnitude from the cumulative distribution function, one can predict the percentage of time that radio beam bending will remain within a required design criterion. However, each K_p percentile is a statistic based on a finite data sample. A small probability exists that the true distribution differs from the observed distribution. Thus confidence intervals were established to determine within which percentile limits the true K_p value would be located given a desired degree of confidence. This same K_p confidence interval defines the range within which K_p will occur for the stated confidence level. Two confidence levels of interest to USACC are 90 and 99 percent. The outermost plots of figures 6 and 7 are the 99 percent confidence limit boundaries, while the intermediate plots are the 90 percent confidence interval boundaries. The interval widths are based on the following nonparametric statistical technique [7].

If $K_1\ K_2 \ldots K_n$ represent an ordered sample of independent random variables with

$$K_1 \leq K_2 \leq \ldots \leq K_r \leq \ldots \leq K_s \leq \ldots K_n$$

and $1 \leq r \leq s \leq n$; then the lower confidence limit is given by

$$r = np - W\,\alpha/2\ \sqrt{np(1 - p)}\ ; \qquad (12)$$

TABLE 2. EXTREME EFFECTIVE EARTH RADIUS K FACTORS

Balboa, Panama		Wiesbaden, Germany	
Cumulative Percent*	K	Cumulative Percent*	K
0.02	-0.10	0.02	-0.73
0.04	-0.17	0.04	-0.75
0.06	-0.18	0.06	-2.12
0.08	-0.18	0.08	-3.20
0.10	-0.25	0.10	-3.49
0.12	-0.26	99.88	0.55
0.14	-0.33	99.90	0.55
0.16	-0.37	99.92	0.52
0.18	-0.41	99.94	0.50
0.20	-0.42	99.96	0.43
0.22	-0.43	99.98	0.40
0.24	-0.57	100.00	0.36
99.87	-0.58		
99.90	0.55		
99.92	0.55		
99.94	0.54		
99.96	0.48		
99.98	0.48		
100.00	0.39		

**Cumulative percentages are based on data listed here and that shown in figures 5 and 6.*

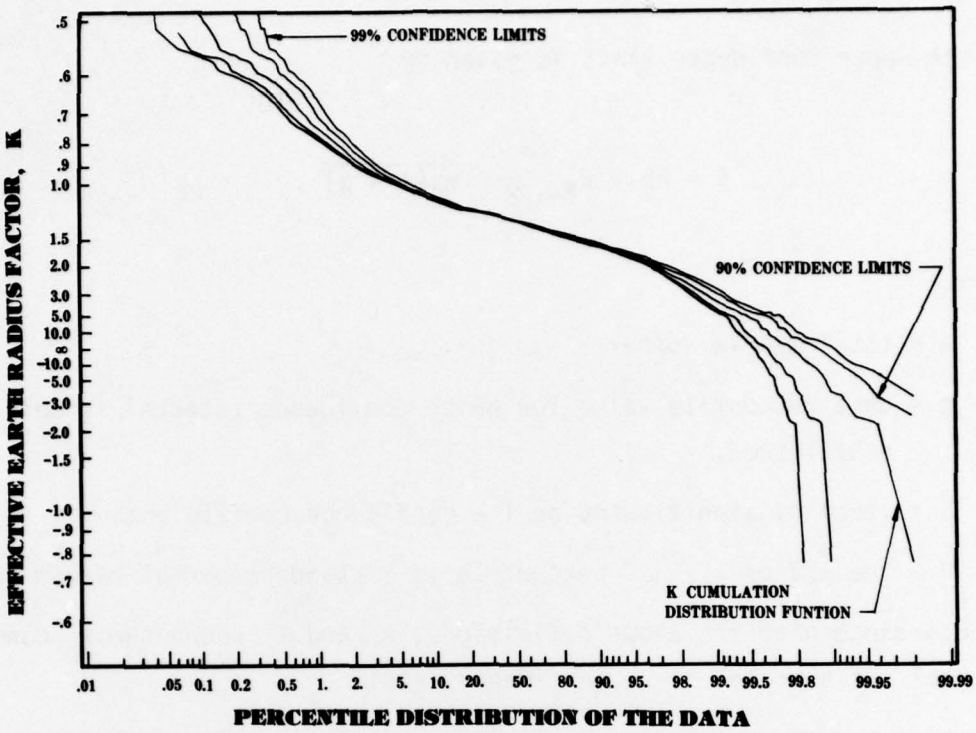

Figure 7. Effective earth radius factor cumulative distribution function and confidence intervals for Wiesbaden, Germany.

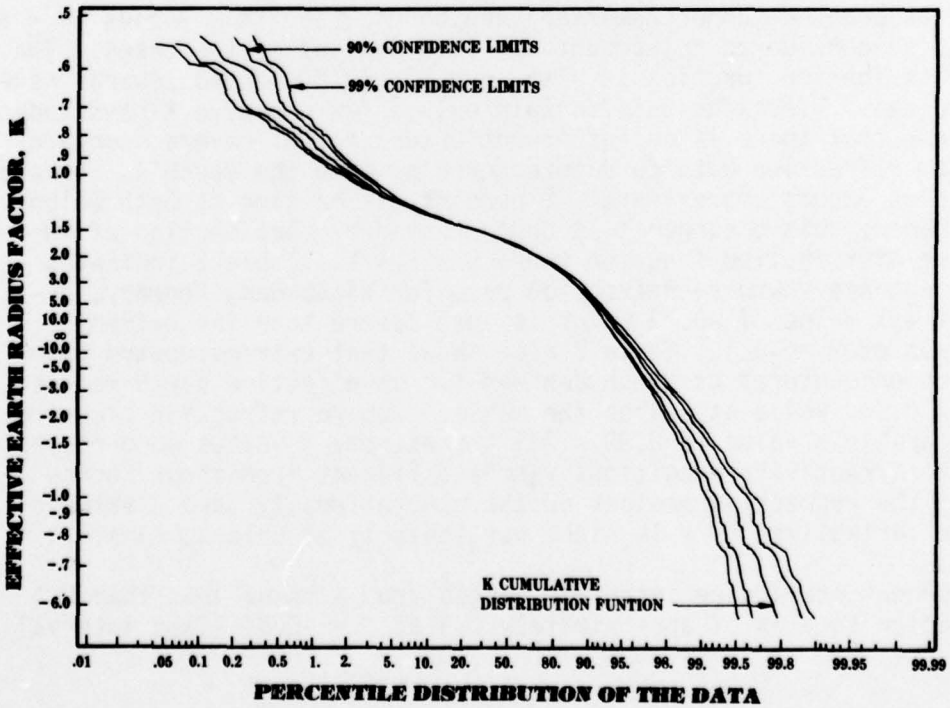

Figure 6. Effective earth radius factor cumulative distribution function and confidence intervals for Balboa, Panama.

and the upper confidence limit is given by

$$S = np + W_{1-\alpha/2} \sqrt{np(1 - p)} , \qquad (13)$$

where

n = total sample number,

p = data percentile value for which confidence interval is being established,

α = level of significance or 1 - confidence coefficient,

W = the $\alpha/2$ or $1 - \alpha/2$ percentile of a standard normal random variable.

In accordance with the above definitions, K_s and K_r bound the K_p confidence interval for a stated $1 - \alpha$ confidence level.

Examination of the cumulative distribution curves in figures 6 and 7 again reveals a higher variability in effective earth radius factor at Balboa. At Wiesbaden, 99.86 percent of the effective earth radius factors encountered can be accounted for by considering the region $0.5 < K \leq \infty$ plus $-\infty \leq K < -2$, while at Balboa the larger numerical region of $0.55 < K \leq \infty$ plus $-\infty \leq K < 0.58$ must be considered to account for 99.7 percent of the cases. The Balboa distribution function is also more widely dispersed towards negative K values. Wiesbaden data contain only a few negative K magnitudes, which means that there is an infrequent occurrence of severe downward radio beam refraction with curvatures greater than the earth's. Upward beam bending occurs approximately 2 percent of the time at both Balboa and Wiesbaden; this occurrence is demonstrated by that section of the cumulative distribution function where $0 < K < 1$. Table 2 indicates that the extreme downward refraction case for Wiesbaden, Germany, occurred at a K value of -0.73 which is less severe than the extreme Balboa case of K = -0.1. Table 2 also shows that extreme upward beam refraction encountered at Wiesbaden was for an effective earth radius factor of 0.36, while at Balboa the maximum upward refraction occurred at a comparable K value of 0.39. All the extreme K values encountered represent refractivity conditions vastly different from those represented by the respective medians or the conventionally used K value of 4/3. The variability of K is high, particularly at Balboa, Panama.

The 99 percent confidence intervals ranged from a ΔK of less than 0.1 at the median to a ΔK of approximately 0.6 at K = -0.89 (last interval

shown on figure 6 graph) for Balboa, and from a ΔK of approximately 0.1 at the median to a ΔK of about 4.3 at K = -2.0 for Wiesbaden. Since effective earth radius factor median changes less than 0.1 are considered negligible for present average microwave communications path lengths, a 99 percent level of confidence can be attached to the fact that the actual medians, both at Balboa and Wiesbaden, will remain ±0.05 K of the calculated median. In contrast, the confidence intervals at the fringe K values of -0.89 and -2.0 can be an appreciable percentage of the measured percentile. At Balboa, the negative section of the confidence interval at K = -0.89 is the larger one. The magnitude is +0.58 and is 35 percent of the absolute value of -0.89. Similarly at Wiesbaden the larger section of the confidence interval has a magnitude of approximately -3 or 150 percent of -2. The significance of these percentages is dependent on the circuit design criteria which define the necessity to keep the refractivity within certain bounds. Confidence intervals for the extreme K values at Wiesbaden are noted to be wider than those at Panama. The relative scarcity or infrequent occurrence of extreme K values at Wiesbaden caused the confidence interval to diverge. Equations 12 and 13 indicate that the width of the interval is dependent on the location of K_r and K_s percentile points. The locations of the K_r and K_s percentiles are dependent on the number of data points available in the K_p vicinity. Consequently, at Panama where the higher K variability places more data points at the fringe area, a smaller interval defines the 90 and 99 percent limits. At Wiesbaden a larger interval is required to retain the same confidence levels. Confidence intervals for the effective earth radius factor data listed in table 2 were not derived because the limited data sample in this data group rendered meaningless statistical results.

CONCLUSIONS

Based on an Army requirement to better understand and quantitatively predict the degree of effective earth radius factor, K, variability, meteorological data were acquired from two distinct locations and used to derive the K factors, which served as test cases. Two areas of concern to USACC-EMEO, Germany and Panama, were chosen as the sample sites. Specifically, atmospheric pressure, temperature, and relative humidity data from Balboa, Panama, and Wiesbaden, Germany, were converted to average refractivity gradients over the first 100 m altitude with the use of an interpolation scheme. Thereafter for each refractivity gradient, a corresponding effective earth radius factor was computed. The median refractivity gradients were determined to be -38 units/km for Wiesbaden and -64 units/km for Balboa. The refractivity gradient distribution was found to be non-Gaussian in both cases. Ninety-five percent of the Balboa refractivity gradients are contained within -202 units/km and -1 unit/km, while at Wiesbaden 95 percent of the data is within -86 units/km and +16 units/km. Median effective earth radius

factors were found to be 1.32 for Wiesbaden and 1.68 for Balboa. Although the Wiesbaden K median is in general agreement with the current "standard" K = 4/3 magnitude, the Balboa K median is significantly different. Median K values for 84 other world locations, listed in table 1, demonstrate the K factor median variability throughout the world. Derived K factors enclosing 68.3, 95.4, 99.7, and 100 percent of the Balboa and Wiesbaden K data, listed in figures 4 and 5 along with the corresponding equivalent earth profiles curves, illustrate the high variability in microwave refraction at these two locations. At Wiesbaden radio beam upward refraction was found to occur 4.6 percent of the time, while downward beam bending occurred 95.4 percent. At Balboa upward refraction occurred only 2.5 percent of the time, while downward refraction occurred the other 97.5 percent of the time. Downward beam refraction is found to be more severe at Balboa. K factor cumulative distribution functions, shown in figures 6 and 7, also demonstrate the K variability at both locations. Boundaries defining the 90 and 99 percent confidence limits of the cumulative distributions established that both medians can be predicted to occur within $K < 0.1$ with a 99 percent level of confidence. Confidence intervals for extreme K values are considerably wider than 0.1 K. In general K was found to be highly variable at both Wiesbaden and Balboa.

Utilization of actual K medians at individual locations instead of the "standard" 4/3 value is recommended when paths are being established for microwave circuits. Such a change should enhance circuit reliability. Equivalent earth profile curves for various possible K values are provided for use as a test design tool. K factor cumulative distribution functions with two confidence interval boundaries are included as a decision tool when high reliability circuits are being prepared.

REFERENCES

1. "Propagation Engineering Services," 1977, Tech Memorandum EMEO-PED-TM-77-3, US Army Communications-Electronics Engineering Installation Agency, Fort Huachuca, Arizona.

2. Letter, dated 9 Feb 77, "Atmospheric Models for Electromagnetic Engineering Predictions," US Army Communications Electronics Installation Agency to Atmospheric Sciences Laboratory, USAECOM.

3. Samson, C. A., 1975, "Refractivity Gradients in the Northern Hemisphere," Office of Telecommunications Report 75-59, Department of Commerce.

4. Bean, B. R., and E. J. Dutton, 1966, Radio Meteorology, US Government Printing Office, Washington, DC.

5. Bean, B. R., and G. D. Thayer, 1959, "Models of the Atmospheric Index of Refraction," Proc. IRE 47, No. 5, 740-755.

6. "Engineering Considerations for Microwave Communications Systems," 1970, Lenkurt Electric Co., Inc., San Carlos, California.

7. Conner, W. J., 1971, Practical Nonparametric Statistics, John Wiley and Sons, Inc., New York.

DISTRIBUTION LIST

Dr. Frank D. Eaton
Geophysical Institute
University of Alaska
Fairbanks, AK 99701

Commander
US Army Aviation Center
ATTN: ATZQ-D-MA
Fort Rucker, AL 36362

Chief, Atmospheric Sciences Div
Code ES-81
NASA
Marshall Space Flight Center,
AL 35812

Commander
US Army Missile R&D Command
ATTN: DRDMI-CGA (B. W. Fowler)
Redstone Arsenal, AL 35809

Redstone Scientific Information Center
ATTN: DRDMI-TBD
US Army Missile R&D Command
Redstone Arsenal, AL 35809

Commander
US Army Missile R&D Command
ATTN: DRDMI-TEM (R. Haraway)
Redstone Arsenal, AL 35809

Commander
US Army Missile R&D Command
ATTN: DRDMI-TRA (Dr. Essenwanger)
Redstone Arsenal, AL 35809

Commander
HQ, Fort Huachuca
ATTN: Tech Ref Div
Fort Huachuca, AZ 85613

Commander
US Army Intelligence Center & School
ATTN: ATSI-CD-MD
Fort Huachuca, AZ 85613

Commander
US Army Yuma Proving Ground
ATTN: Technical Library
Bldg 2100
Yuma, AZ 85364

Naval Weapons Center (Code 3173)
ATTN: Dr. A. Shlanta
China Lake, CA 93555

Sylvania Elec Sys Western Div
ATTN: Technical Reports Library
PO Box 205
Mountain View, CA 94040

Geophysics Officer
PMTC Code 3250
Pacific Missile Test Center
Point Mugu, CA 93042

Commander
Naval Ocean Systems Center (Code 4473)
ATTN: Technical Library
San Diego, CA 92152

Meteorologist in Charge
Kwajalein Missile Range
PO Box 67
APO San Francisco, 96555

Director
NOAA/ERL/APCL R31
RB3-Room 567
Boulder, CO 80302

Library-R-51-Tech Reports
NOAA/ERL
320 S. Broadway
Boulder, CO 80302

National Center for Atmos Research
NCAR Library
PO Box 3000
Boulder, CO 80307

B. Girardo
Bureau of Reclamation
E&R Center, Code 1220
Denver Federal Center, Bldg 67
Denver, CO 80225

National Weather Service
National Meteorological Center
W321, WWB, Room 201
ATTN: Mr. Quiroz
Washington, DC 20233

Mil Assistant for Atmos Sciences
Ofc of the Undersecretary of Defense
for Rsch & Engr/E&LS - Room 3D129
The Pentagon
Washington, DC 20301

Defense Communications Agency
Technical Library Center
Code 205
Washington, DC 20305

Director
Defense Nuclear Agency
ATTN: Technical Library
Washington, DC 20305

HQDA (DAEN-RDM/Dr. de Percin)
Washington, DC 20314

Director
Naval Research Laboratory
Code 5530
Washington, DC 20375

Commanding Officer
Naval Research Laboratory
Code 2627
Washington, DC 20375

Dr. J. M. MacCallum
Naval Research Laboratory
Code 1409
Washington, DC 20375

The Library of Congress
ATTN: Exchange & Gift Div
Washington, DC 20540
2

Head, Atmos Rsch Section
Div Atmospheric Science
National Science Foundation
1800 G. Street, NW
Washington, DC 20550

CPT Hugh Albers, Exec Sec
Interdept Committee on Atmos Science
National Science Foundation
Washington, DC 20550

Director, Systems R&D Service
Federal Aviation Administration
ATTN: ARD-54
2100 Second Street, SW
Washington, DC 20590

ADTC/DLODL
Eglin AFB, FL 32542

Naval Training Equipment Center
ATTN: Technical Library
Orlando, FL 32813

Det 11, 2WS/OI
ATTN: Maj Orondorff
Patrick AFB, FL 32925

USAFETAC/CB
Scott AFB, IL 62225

HQ, ESD/TOSI/S-22
Hanscom AFB, MA 01731

Air Force Geophysics Laboratory
ATTN: LCB (A. S. Carten, Jr.)
Hanscom AFB, MA 01731

Air Force Geophysics Laboratory
ATTN: LYD
Hanscom AFB, MA 01731

Meteorology Division
AFGL/LY
Hanscom AFB, MA 01731

US Army Liaison Office
MIT-Lincoln Lab, Library A-082
PO Box 73
Lexington, MA 02173

Director
US Army Ballistic Rsch Lab
ATTN: DRDAR-BLB (Dr. G. E. Keller)
Aberdeen Proving Ground, MD 21005

Commander
US Army Ballistic Rsch Lab
ATTN: DRDAR-BLP
Aberdeen Proving Ground, MD 21005

Director
US Army Armament R&D Command
Chemical Systems Laboratory
ATTN: DRDAR-CLJ-I
Aberdeen Proving Ground, MD 21010

Chief CB Detection & Alarms Div
Chemical Systems Laboratory
ATTN: DRDAR-CLC-CR (H. Tannenbaum)
Aberdeen Proving Ground, MD 21010

Commander
Harry Diamond Laboratories
ATTN: DELHD-CO
2800 Powder Mill Road
Adelphi, MD 20783

Commander
ERADCOM
ATTN: DRDEL-AP
2800 Powder Mill Road
Adelphi, MD 20783
2

Commander
ERADCOM
ATTN: DRDEL-CG/DRDEL-DC/DRDEL-CS
2800 Powder Mill Road
Adelphi, MD 20783

Commander
ERADCOM
ATTN: DRDEL-CT
2800 Powder Mill Road
Adelphi, MD 20783

Commander
ERADCOM
ATTN: DRDEL-EA
2800 Powder Mill Road
Adelphi, MD 20783

Commander
ERADCOM
ATTN: DRDEL-PA/DRDEL-ILS/DRDEL-E
2800 Powder Mill Road
Adelphi, MD 20783

Commander
ERADCOM
ATTN: DRDEL-PAO (S. Kimmel)
2800 Powder Mill Road
Adelphi, MD 20783

Chief
Intelligence Materiel Dev & Support Ofc
ATTN: DELEW-WL-I
Bldg 4554
Fort George G. Meade, MD 20755

Acquisitions Section, IRDB-D823
Library & Info Service Div, NOAA
6009 Executive Blvd
Rockville, MD 20852

Naval Surface Weapons Center
White Oak Library
Silver Spring, MD 20910

The Environmental Research
Institute of MI
ATTN: IRIA Library
PO Box 8618
Ann Arbor, MI 48107

Mr. William A. Main
USDA Forest Service
1407 S. Harrison Road
East Lansing, MI 48823

Dr. A. D. Belmont
Research Division
PO Box 1249
Control Data Corp
Minneapolis, MN 55440

Director
Naval Oceanography & Meteorology
NSTL Station
Bay St Louis, MS 39529

Director
US Army Engr Waterways Experiment Sta
ATTN: Library
PO Box 631
Vicksburg, MS 39180

Commander
US Army Dugway Proving Ground
ATTN: STEDP-MT-DA-M (Mr. Paul Carlson)
Dugway, UT 84022

Commander
TRASANA
ATTN: DELAS-ATAA-PL
(Dolores Anguiano)
White Sands Missile Range, NM 88002

ATMOSPHERIC SCIENCES RESEARCH PAPERS

1. Lindberg, J.D., "An Improvement to a Method for Measuring the Absorption Coefficient of Atmospheric Dust and other Strongly Absorbing Powders, " ECOM-5565, July 1975.
2. Avara, Elton, P., "Mesoscale Wind Shears Derived from Thermal Winds," ECOM-5566, July 1975.
3. Gomez, Richard B., and Joseph H. Pierluissi, "Incomplete Gamma Function Approximation for King's Strong-Line Transmittance Model," ECOM-5567, July 1975.
4. Blanco, A.J., and B.F. Engebos, "Ballistic Wind Weighting Functions for Tank Projectiles," ECOM-5568, August 1975.
5. Taylor, Fredrick J., Jack Smith, and Thomas H. Pries, "Crosswind Measurements through Pattern Recognition Techniques," ECOM-5569, July 1975.
6. Walters, D.L., "Crosswind Weighting Functions for Direct-Fire Projectiles," ECOM-5570, August 1975.
7. Duncan, Louis D., "An Improved Algorithm for the Iterated Minimal Information Solution for Remote Sounding of Temperature," ECOM-5571, August 1975.
8. Robbiani, Raymond L., "Tactical Field Demonstration of Mobile Weather Radar Set AN/TPS-41 at Fort Rucker, Alabama," ECOM-5572, August 1975.
9. Miers, B., G. Blackman, D. Langer, and N. Lorimier, "Analysis of SMS/GOES Film Data," ECOM-5573, September 1975.
10. Manquero, Carlos, Louis Duncan, and Rufus Bruce, "An Indication from Satellite Measurements of Atmospheric CO2 Variability," ECOM-5574, September 1975.
11. Petracca, Carmine, and James D. Lindberg, "Installation and Operation of an Atmospheric Particulate Collector," ECOM-5575, September 1975.
12. Avara, Elton P., and George Alexander, "Empirical Investigation of Three Iterative Methods for Inverting the Radiative Transfer Equation," ECOM-5576, October 1975.
13. Alexander, George D., "A Digital Data Acquisition Interface for the SMS Direct Readout Ground Station — Concept and Preliminary Design," ECOM-5577, October 1975.
14. Cantor, Israel, "Enhancement of Point Source Thermal Radiation Under Clouds in a Nonattenuating Medium," ECOM-5578, October 1975.
15. Norton, Colburn, and Glenn Hoidale, "The Diurnal Variation of Mixing Height by Month over White Sands Missile Range, N.M," ECOM-5579, November 1975.
16. Avara, Elton P., "On the Spectrum Analysis of Binary Data," ECOM-5580, November 1975.
17. Taylor, Fredrick J., Thomas H. Pries, and Chao-Huan Huang, "Optimal Wind Velocity Estimation," ECOM-5581, December 1975.
18. Avara, Elton P., "Some Effects of Autocorrelated and Cross-Correlated Noise on the Analysis of Variance, " ECOM-5582, December 1975.
19. Gillespie, Patti S., R.L. Armstrong, and Kenneth O. White, "The Spectral Characteristics and Atmospheric CO2 Absorption of the Ho^{+3}:YLF Laser at 2.05μm," ECOM-5583, December 1975.
20. Novlan, David J. "An Empirical Method of Forecasting Thunderstorms for the White Sands Missile Range," ECOM-5584, February 1976.
21. Avara, Elton P., "Randomization Effects in Hypothesis Testing with Autocorrelated Noise," ECOM-5585, February 1976.
22. Watkins, Wendell R., "Improvements in Long Path Absorption Cell Measurement," ECOM-5586, March 1976.
23. Thomas, Joe, George D. Alexander, and Marvin Dubbin, "SATTEL — An Army Dedicated Meteorological Telemetry System," ECOM-5587. March 1976.
24. Kennedy, Bruce W., and Delbert Bynum, "Army User Test Program for the RDT&E-XM-75 Meteorological Rocket," ECOM-5588, April 1976.

25. Barnett, Kenneth M., "A Description of the Artillery Meteorological Comparisons at White Sands Missle Range, October 1974 - December 1974 ('PASS' - Prototype Artillery [Meteorological] Subsystem)," ECOM-5589, April 1976.
26. Miller, Walter B., "Preliminary Analysis of Fall-of-Shot From Project 'PASS'," ECOM-5590, April 1976.
27. Avara, Elton P., "Error Analysis of Minimum Information and Smith's Direct Methods for Inverting the Radiative Transfer Equation," ECOM-5591, April 1976.
28. Yee, Young P., James D. Horn, and George Alexander, "Synoptic Thermal Wind Calculations from Radiosonde Observations Over the Southwestern United States," ECOM-5592, May 1976.
29. Duncan, Louis D., and Mary Ann Seagraves, "Applications of Empirical Corrections to NOAA-4 VTPR Observations," ECOM-5593, May 1976.
30. Miers, Bruce T., and Steve Weaver, "Applications of Meterological Satellite Data to Weather Sensitive Army Operations,"ECOM-5594, May 1976.
31. Sharenow, Moses, "Redesign and Improvement of Balloon ML-566," ECOM-5595, June, 1976.
32. Hansen, Frank V., "The Depth of the Surface Boundary Layer," ECOM-5596, June 1976.
33. Pinnick, R.G., and E.B. Stenmark, "Response Calculations for a Commercial Light-Scattering Aerosol Counter," ECOM-5597, July 1976.
34. Mason, J., and G.B. Hoidale, "Visibility as an Estimator of Infrared Transmittance," ECOM-5598, July 1976.
35. Bruce, Rufus E., Louis D. Duncan, and Joseph H. Pierluissi, "Experimental Study of the Relationship Between Radiosonde Temperatures and Radiometric-Area Temperatures," ECOM-5599, August 1976.
36. Duncan, Louis D., "Stratospheric Wind Shear Computed from Satellite Thermal Sounder Measurements," ECOM-5800, September 1976.
37. Taylor, F., P. Mohan, P. Joseph and T. Pries, "An All Digital Automated Wind Measurement System," ECOM-5801, September 1976.
38. Bruce, Charles, "Development of Spectrophones for CW and Pulsed Radiation Sources," ECOM-5802, September 1976.
39. Duncan, Louis D., and Mary Ann Seagraves,"Another Method for Estimating Clear Column Radiances," ECOM-5803, October 1976.
40. Blanco, Abel J., and Larry E. Taylor, "Artillery Meteorological Analysis of Project Pass," ECOM-5804, October 1976.
41. Miller, Walter, and Bernard Engebos," A Mathematical Structure for Refinement of Sound Ranging Estimates," ECOM-5805, November, 1976.
42. Gillespie, James B., and James D. Lindberg, "A Method to Obtain Diffuse Reflectance Measurements from 1.0 to 3.0 μm Using a Cary 17I Spectrophotometer," ECOM-5806, November 1976.
43. Rubio, Roberto, and Robert O. Olsen,"A Study of the Effects of Temperature Variations on Radio Wave Absorption,"ECOM-5807, November 1976.
44. Ballard, Harold N., "Temperature Measurements in the Stratosphere from Balloon-Borne Instrument Platforms, 1968-1975," ECOM-5808, December 1976.
45. Monahan, H.H., "An Approach to the Short-Range Prediction of Early Morning Radiation Fog," ECOM-5809, January 1977.
46. Engebos, Bernard Francis, "Introduction to Multiple State Multiple Action Decision Theory and Its Relation to Mixing Structures," ECOM-5810, January 1977.
47. Low, Richard D.H.,"Effects of Cloud Particles on Remote Sensing from Space in the 10-Micrometer Infrared Region," ECOM-5811, January 1977.
48. Bonner, Robert S., and R. Newton, "Application of the AN/GVS-5 Laser Rangefinder to Cloud Base Height Measurements," ECOM-5812, February 1977.
49. Rubio, Roberto, "Lidar Detection of Subvisible Reentry Vehicle Erosive Atmospheric Material," ECOM-5813, March 1977.
50. Low, Richard D.H., and J.D. Horn, "Mesoscale Determination of Cloud-Top Height: Problems and Solutions," ECOM-5814, March 1977.

51. Duncan, Louis D., and Mary Ann Seagraves,"Evaluation of the NOAA-4 VTPR Thermal Winds for Nuclear Fallout Predictions," ECOM-5815, March 1977.
52. Randhawa, Jagir S., M. Izquierdo, Carlos McDonald and Zvi Salpeter, "Stratospheric Ozone Density as Measured by a Chemiluminescent Sensor During the Stratcom VI-A Flight," ECOM-5816, April 1977.
53. Rubio, Roberto, and Mike Izquierdo, "Measurements of Net Atmospheric Irradiance in the 0.7- to 2.8-Micrometer Infrared Region," ECOM-5817, May 1977.
54. Ballard, Harold N., Jose M. Serna, and Frank P. Hudson Consultant for Chemical Kinetics, "Calculation of Selected Atmospheric Composition Parameters for the Mid-Latitude, September Stratosphere," ECOM-5818, May 1977.
55. Mitchell, J.D., R.S. Sagar, and R.O. Olsen, "Positive Ions in the Middle Atmosphere During Sunrise Conditions," ECOM-5819, May 1977.
56. White, Kenneth O., Wendell R. Watkins, Stuart A. Schleusener, and Ronald L. Johnson, "Solid-State Laser Wavelength Identification Using a Reference Absorber," ECOM-5820, June 1977.
57. Watkins, Wendell R., and Richard G. Dixon, "Automation of Long-Path Absorption Cell Measurements," ECOM-5821, June 1977.
58. Taylor, S.E., J.M. Davis, and J.B. Mason, "Analysis of Observed Soil Skin Moisture Effects on Reflectance," ECOM-5822, June 1977.
59. Duncan, Louis D. and Mary Ann Seagraves, "Fallout Predictions Computed from Satellite Derived Winds," ECOM-5823. June 1977.
60. Snider, D.E., D.G. Murcray, F.H. Murcray, and W.J. Williams, "Investigation of High-Altitude Enhanced Infrared Backround Emissions" (U), SECRET, ECOM-5824, June 1977.
61. Dubbin, Marvin H. and Dennis Hall, "Synchronous Meteorlogical Satellite Direct Readout Ground System Digital Video Electronics," ECOM-5825, June 1977.
62. Miller, W., and B. Engebos, "A Preliminary Analysis of Two Sound Ranging Algorithms," ECOM-5826, July 1977.
63. Kennedy, Bruce W., and James K. Luers, "Ballistic Sphere Techniques for Measuring Atomspheric Parameters," ECOM-5827, July 1977.
64. Duncan, Louis D., "Zenith Angle Variation of Satellite Thermal Sounder Measurements," ECOM-5828, August 1977.
65. Hansen, Frank V., "The Critical Richardson Number," ECOM-5829, September 1977.
66. Ballard, Harold N., and Frank P. Hudson (Compilers), "Stratospheric Composition Balloon-Borne Experiment," ECOM-5830, October 1977.
67. Barr, William C., and Arnold C. Peterson, "Wind Measuring Accuracy Test of Meteorological Systems," ECOM-5831, November 1977.
68. Ethridge, G.A. and F.V. Hansen, "Atmospheric Diffusion: Similarity Theory and Empirical Derivations for Use in Boundary Layer Diffusion Problems," ECOM-5832, November 1977.
69. Low, Richard D.H., "The Internal Cloud Radiation Field and a Technique for Determining Cloud Blackness," ECOM-5833, December 1977.
70. Watkins, Wendell R., Kenneth O. White, Charles W. Bruce, Donald L. Walters, and James D. Lindberg, "Measurements Required for Prediction of High Energy Laser Transmission," ECOM-5834, December 1977.
71. Rubio, Robert, "Investigation of Abrupt Decreases in Atmospherically Backscattered Laser Energy," ECOM-5835. December 1977.
72. Monahan, H.H. and R.M. Cionco, "An Interpretative Review of Existing Capabilities for Measuring and Forecasting Selected Weather Variables (Emphasizing Remote Means)," ASL-TR-0001, January 1978.
73. Heaps, Melvin G., "The 1979 Solar Eclipse and Validation of D-Region Models," ASL-TR-0002. March 1978.

74. Jennings, S.G., and J.B. Gillespie, "M.I.E. Theory Sensitivity Studies - The Effects of Aerosol Complex Refractive Index and Size Distribution Variations on Extinction and Absorption Coefficients Part II: Analysis of the Computational Results," ASL-TR-0003, March 1978.
75. White, Kenneth O. et al, "Water Vapor Continuum Absorption in the 3.5μm to 4.0μm Region," ASL-TR-0004, March 1978.
76. Olsen, Robert O., and Bruce W. Kennedy, "ABRES Pretest Atmospheric Measurements," ASL-TR-0005, April 1978.
77. Ballard, Harold N., Jose M. Serna, and Frank P. Hudson, "Calculation of Atmospheric Composition in the High Latitude September Stratosphere," ASL-TR-0006, May 1978.
78. Watkins, Wendell R. et al, "Water Vapor Absorption Coefficients at HF Laser Wavelengths," ASL-TR-0007, May 1978.
79. Hansen, Frank V., "The Growth and Prediction of Nocturnal Inversions," ASL-TR-0008, May 1978.
80. Samuel, Christine, Charles Bruce, and Ralph Brewer, "Spectrophone Analysis of Gas Samples Obtained at Field Site," ASL-TR-0009, June 1978.
81. Pinnick, R.G. et al., "Vertical Structure in Atmospheric Fog and Haze and its Effects on IR Extinction," ASL-TR-0010, July 1978.
82. Low, Richard D.H., Louis D. Duncan, and Richard B. Gomez, "The Microphysical Basis of Fog Optical Characterization," ASL-TR-0011, August 1978.
83. Heaps, Melvin G., "The Effect of a Solar Proton Event on the Minor Neutral Constituents of the Summer Polar Mesosphere," ASL-TR-0012, August 1978.
84. Mason, James B., "Light Attenuation in Falling Snow," ASL-TR-0013, August 1978.
85. Blanco, Abel J., "Long-Range Artillery Sound Ranging: "PASS" Meteorological Application," ASL-TR-0014, September 1978.
86. Heaps, M.G., and F.E. Niles, "Modeling the Ion Chemistry of the D-Region: A case Study Based Upon the 1966 Total Solar Eclipse," ASL-TR-0015, September 1978.
87. Jennings, S.G., and R.G. Pinnick, "Effects of Particulate Complex Refractive Index and Particle Size Distribution Variations on Atmospheric Extinction and Absorption for Visible Through Middle-Infrared Wavelengths," ASL-TR-0016, September 1978.
88. Watkins, Wendell R., Kenneth O. White, Lanny R. Bower, and Brian Z. Sojka, " Pressure Dependence of the Water Vapor Continuum Absorption in the 3.5- to 4.0-Micrometer Region," ASL-TR-0017, September 1978.
89. Miller, W.B., and B.F. Engebos, "Behavior of Four Sound Ranging Techniques in an Idealized Physical Enviroment," ASL-TR-0018, September 1978.
90. Gomez, Richard G., "Effectiveness Studies of the CBU-88/B Bomb, Cluster, Smoke Weapon" (U), CONFIDENTIAL ASL-TR-0019, September 1978.
91. Miller, August, Richard C. Shirkey, and Mary Ann Seagraves, "Calculation of Thermal Emission from Aerosols Using the Doubling Technique," ASL-TR-0020, November, 1978.
92. Lindberg, James D. et al., "Measured Effects of Battlefield Dust and Smoke on Visible, Infrared, and Millimeter Wavelengths Propagation: A Preliminary Report on Dusty Infrared Test-I (DIRT-I)," ASL-TR-0021, January 1979.
93. Kennedy, Bruce W., Arthur Kinghorn, and B.R. Hixon, "Engineering Flight Tests of Range Meteorological Sounding System Radiosonde," ASL-TR-0022, February 1979.
94. Rubio, Roberto, and Don Hoock, "Microwave Effective Earth Radius Factor Variability at Wiesbaden and Balboa," ASL-TR-0023, February 1979.

☆U.S. GOVERNMENT PRINTING OFFICE: 1979 677-017/29